Organic & Biomolecular Chemistry

Dynamic Article Links

Cite this: *Org. Biomol. Chem.*, 2011, **9**, 7822

www.rsc.org/obc

PAPER

Synthesis and oxidation of 2-hydroxynevirapine, a metabolite of the HIV reverse transcriptase inhibitor nevirapine†

Alexandra M. M. Antunes,*[a] David A. Novais,[a] J. L. Ferreira da Silva,[a] Pedro P. Santos,[a] M. Conceição Oliveira,[a] Frederick A. Beland[b] and M. Matilde Marques*[a]

Received 30th June 2011, Accepted 18th August 2011
DOI: 10.1039/c1ob06052j

Nevirapine (11-cyclopropyl-5,11-dihydro-4-methyl-6*H*-dipyrido[3,2-b:2′,3′-e][1,4]diazepin-6-one, NVP) is a non-nucleoside HIV-1 reverse transcriptase inhibitor used to prevent mother-to-child transmission of the virus. However, severe hepatotoxicity and serious adverse cutaneous effects have raised concerns about the safety of NVP administration. NVP metabolism yields several phenol-type derivatives conceivably capable of undergoing further metabolic oxidation to electrophilic quinoid species that could react with bionucleophiles. The covalent adducts thus formed might be at the genesis of toxic responses. As an initial step to test this hypothesis, we synthesized the phenolic metabolite, 2-hydroxy-NVP, and investigated its oxidation *in vitro*. Using potassium nitrosodisulfonate and sodium periodate as model oxidants, we obtained evidence for fast generation of an electrophilic quinone-imine, which readily underwent hydrolytic conversion to fully characterized spiro derivatives, 1′-cyclopropyl-4-methyl-1*H*,1′*H*-spiro[pyridine-2,2′-pyrido[2,3-*d*]pyrimidine]-3,4′,6(3′*H*)-trione in aqueous media and 1′-cyclopropyl-4-methyl-1′*H*,2*H*-spiro[pyridine-3,2′-pyrido[2,3-*d*]pyrimidine]-2,4′,6(1*H*,3′*H*)-trione in non-aqueous media. The spiro compound generated in aqueous solution underwent subsequent hydrolytic degradation of the NVP ring system, whereas the one formed in non-aqueous media was stable to hydrolysis. The product profile observed with the chemical oxidants in aqueous solution was replicated using lactoperoxidase-mediated oxidation of 2-hydroxy-NVP. These observations suggest that metabolic activation of NVP, *via* Phase I oxidation to 2-hydroxy-NVP and subsequent generation of a quinone-imine, could occur *in vivo* and play a role in NVP-induced toxicity.

Introduction

The chronic treatment of individuals infected with the human immunodeficiency virus type 1 (HIV) is expected to remain a vital need in the near future, since both eradication of the virus and an ending to new infections are unlikely scenarios. Despite the indisputable benefits of the currently recommended combined antiretroviral therapy (CART), and although individual susceptibilities differ among patients,[1] concerns with the adverse effects of long-term CART are emerging.[2,3] Thus, an understanding of the molecular mechanisms underlying the toxicity of antiretroviral drugs is essential for establishing dependable risk-benefit relationships that can guide decisions on treatment options.

The starting CART regimens recommended by World Health Organization guidelines typically include a non-nucleoside reverse transcriptase inhibitor (NNRTI).[4] In 1996, nevirapine (11-cyclopropyl-5,11-dihydro-4-methyl-6*H*-dipyrido[3,2-b:2′,3′-e]diazepin-6-one (**1**, NVP, Scheme 1) was the first NNRTI approved by the US FDA for use in combination therapy for HIV-1 infection.[5] The high efficacy levels of the drug, favorable lipid profile, and suitability for use during pregnancy have since granted NVP-based regimens a significant role in HIV-1 treatment strategies.[6,7] Currently, NVP is one of the most prescribed antiretroviral drugs in the developing world, both as a single drug to prevent mother-to-child HIV transmission and as a component of CART.[8–11] While the immediate-release formulation currently on the market is approved for twice-daily dosing, a more convenient once-daily alternative was approved by the US FDA in March 2011.[12] This new option should be particularly beneficial in resource-limited countries, where adherence is a recurrent problem, and may lead to an increased worldwide use of the drug.

Despite its clinical efficacy and suitability for use during pregnancy[13] and breastfeeding,[14] NVP is associated with a variety of toxic responses. The most severe is hepatotoxicity, which can

[a]*Centro de Química Estrutural, Instituto Superior Técnico, Universidade Técnica de Lisboa, 1049-001, Lisboa, Portugal. E-mail: alexandra.antunes@ist.utl.pt; Tel: 351-21-8419388, matilde.marques@ist.utl.pt; Tel: 351-21-8419200; Fax: 351-21-8464455*

[b]*Division of Biochemical Toxicology, National Center for Toxicological Research, Jefferson, AR 72079, USA*

† Electronic supplementary information (ESI) available: supplementary data and crystallographic data for compound **18**. CCDC reference number 821404. For ESI and crystallographic data in CIF or other electronic format see DOI: 10.1039/c1ob06052j

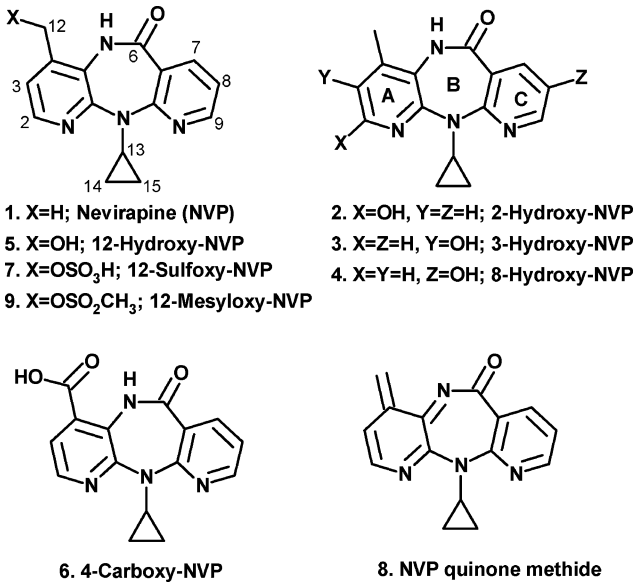

Scheme 1 Structures of NVP (**1**) and the NVP metabolites and derivatives (**2–9**) mentioned in the text.

be fatal; the most common side effect is skin rash, which may be life threatening and lead to drug discontinuation.[15,16] Moreover, although NVP is neither mutagenic nor clastogenic in standard *in vitro* assays, it induces hepatoneoplasias in rodents.[17] In addition, while no direct correlation between NVP administration and the occurrence of cancer in humans has been reported, recent epidemiological data on the incidence of non-AIDS defining cancers in individuals undergoing CART suggest that the use of NNRTIs is a risk factor.[18] These observations raise concerns about prolonged administration of the drug.

While the reasons for the adverse effects of NVP are still unclear, increasing evidence suggests that metabolic activation to highly reactive electrophiles, prone to react with bionucleophiles, has a role in the initiation of the toxic responses. For instance, although circumstantial, the report of fast clinical recovery of a patient suffering from NVP-induced toxic epidermal necrolysis and toxic hepatitis upon treatment with a continuous infusion of human immunoglobulins and a high dose (300 mg day^{-1}) of N-acetylcysteine,[19] supports the involvement of reactive NVP metabolites in the toxic response. Indeed, it is plausible that administration of N-acetylcysteine, an excellent nucleophile, detoxified electrophilic NVP metabolites through the formation of readily excreted mercapturate conjugates.

In all species investigated, cytochrome P450 (CYP)-mediated Phase I metabolism of NVP yields 2-, 3-, 8-, and 12-OH-NVP, and 4-carboxy-NVP (**2–6**, Scheme 1); the majority of these metabolites undergo a detoxifying glucuronidation and subsequent excretion.[20–24] It has been suggested that 12-OH-NVP is the species responsible for a skin rash in rats that resembles the rash in humans,[25,26] and sulfotransferase-catalyzed conversion of 12-OH-NVP into 12-sulfoxy-NVP (**7**), possibly followed by hydrogen sulfate elimination to an NVP quinone methide (**8**), has been proposed as the bioactivation pathway in the process.[25,27] Using 12-mesyloxy-NVP (**9**) as a synthetic surrogate for 12-sulfoxy-NVP, we demonstrated the potential of this species to react *in vitro* with DNA and proteins[28–30] yielding covalent adducts. Evidence for the binding of NVP metabolites to bionucleophiles *in vivo* was presented by Srivastava *et al.*[31] who identified two NVP mercapturates, the major one through NVP-C3 and the minor one through NVP-C12 (**10** and **11**, respectively, Scheme 2), in the urine of HIV-positive patients administered NVP as part of a standard antiretroviral therapeutic regimen. While the minor mercapturate presumably resulted from the previously proposed bioactivation pathway through 12-OH-NVP, it was hypothesized[31] that the formation of the NVP-C3 adduct with *N*-acetylcysteine occurred by nucleophilic attack of glutathione on either the quinone methide **8** or an arene oxide intermediate (**12**, Scheme 2). This report represented the first indication that metabolic pathways other than 12-hydroxylation could have a role in NVP-induced toxicity. In particular, it can not be excluded that the phenolic metabolites (*e.g.*, 2-OH-NVP), generated from CYP-mediated oxidation to arene oxide (*e.g.*, **12**) and/or diradical (*e.g.*, **13**) precursors, may undergo metabolic activation to quinone/semiquinone electrophiles (*e.g.*, **14**) capable of reacting with bionucleophiles through Michael-type addition and/or Schiff-base formation, leading to covalent adduct formation (Scheme 2).[32–34]

To gain insight into the potential role of phenolic metabolites in the toxicity associated with NVP administration, we synthesized 2-OH-NVP and investigated its oxidation *in vitro*. We report herein evidence for the formation of an electrophilic quinone-imine intermediate, using both model chemical oxidants [potassium nitrosodisulfonate (Frémy's salt) and sodium periodate] and lactoperoxidase catalysis.

Results and discussion

Synthesis of 2-OH-NVP

Two distinct methods are reported in the literature for the preparation of 2-OH-NVP (**2**), starting from either NVP or 2-chloro-NVP. However, multiple synthetic steps are involved in both instances, yielding **2** with an overall yield of less than 10%.[35] For the ultimate goal of investigating the oxidation of 2-OH-NVP, it was essential to have a considerable amount of this NVP metabolite; for this reason, our initial efforts focused on the development of a new and more efficient synthetic methodology.

The addition of 8.0 molar equivalents of silver acetate and 4.8 molar equivalents of iodine to an NVP solution in dichloromethane resulted in an efficient method for selective acetoxylation at the aromatic NVP C2, affording 2-acetoxy-NVP (**15**, Scheme 3) after only 10 min of reflux. Upon subsequent hydrolysis, 2-OH-NVP was obtained in an overall 85% yield. This fast and cost-efficient two-step strategy represents a significant improvement when compared with the already available methods for C2 hydroxylation of NVP. The iodine/silver acetate system has found some limited synthetic use, namely in the synthesis of *anti*-[36] and *syn*-diols[37] from alkenes, in the preparation of β-iodoketones,[38] in the acetoxylation of porphyrins,[39] and in the iodination of *N*-heterocycles;[40] however, to the best of our knowledge, this is the first time it is employed for the acetoxylation of a pyridine ring. We found the efficiency of NVP acetoxylation to be strongly dependent on the order of reagent addition. When iodine was the first reagent to be added, acetoxylation was almost negligible, which rules out activation *via* direct nucleophilic attack on iodine,

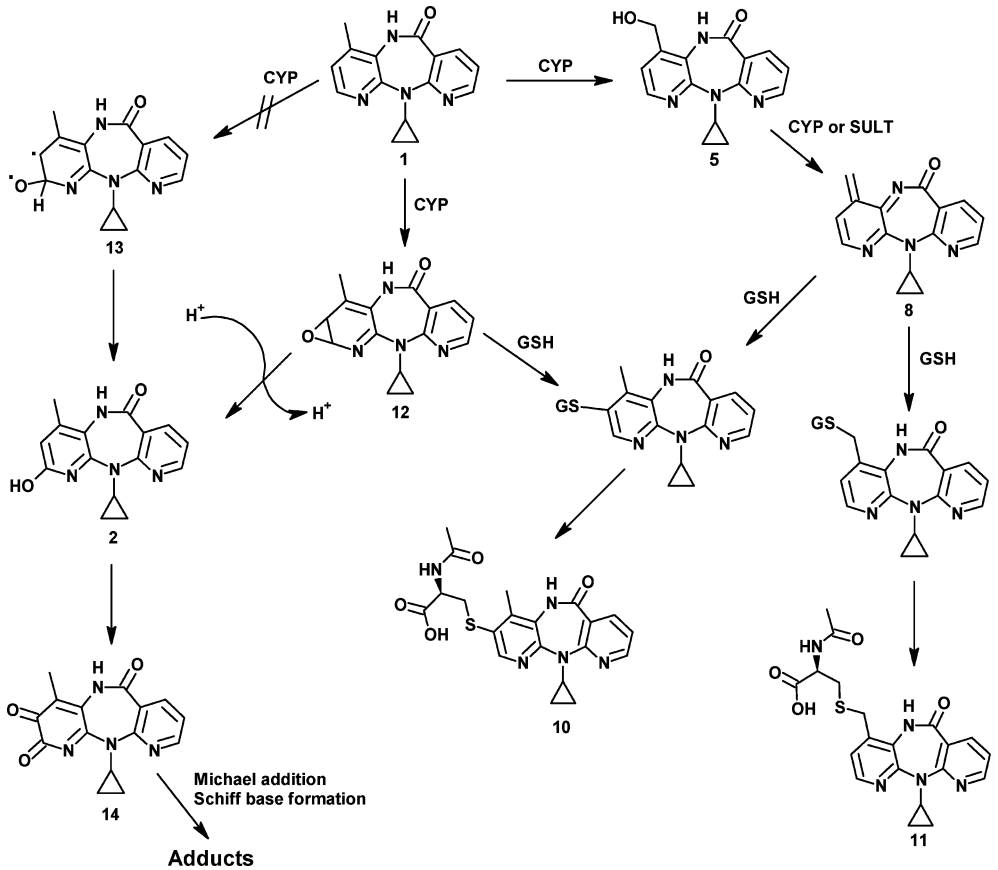

Scheme 2 Hypothetic pathways for *in vivo* generation of covalent adducts from 2-hydroxy-NVP (**2**). GSH, glutathione; SULT, sulfotransferase.

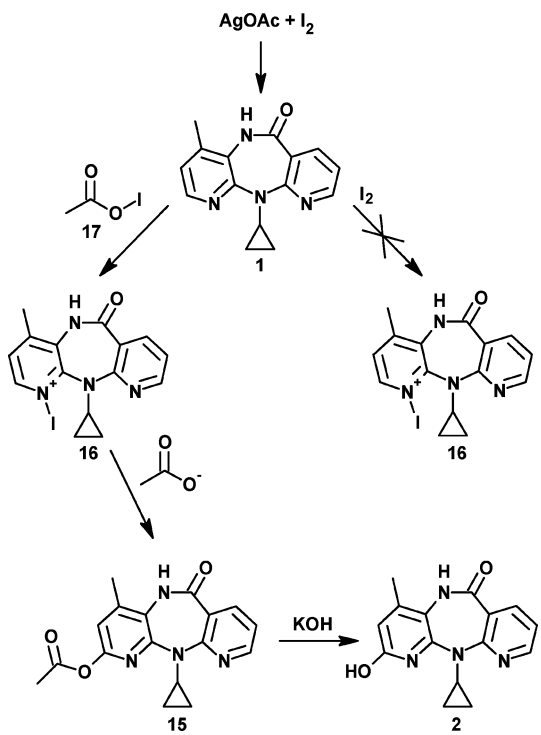

Scheme 3 Proposed mechanism for the synthetic conversion of NVP (**1**) into 2-OH-NVP (**2**).

with formation of an iodopyridinium species (*e.g.* **16**, Scheme 3, or its di-iodo analogue).[41] Our observations suggest an initial reaction of silver acetate with iodine, affording acetyl hypoiodite (**17**), which is a known iodination reagent[42] and alcohol oxidant.[43] The transient formation of this species is consistent with the copious precipitation of a yellow solid (presumed to be silver iodide) after reagent addition, similar to what has been reported by Barnett and co-workers.[42] Moreover, the fact that a similar compound, acetyl hypofluorite, is reported to promote the acetoxylation of pyridine rings[44,45] reinforces this hypothesis. Light-induced homolytic cleavage of the I–O bond in acetyl hypoiodite is reported to occur during alcohol oxidation;[43] however, the formation of 2-acetoxy-NVP also occurred in the dark, which supports an ionic, rather than a free radical, mechanism. Presumably, the iodopyridinium analogue (**16**) was formed by reaction of NVP with acetyl hypoiodite, followed by a Chichibabin-type nucleophilic addition of acetate on the NVP C2 and subsequent HI elimination.[44,45]

Chemical oxidation reactions

The metabolic oxidation of 2-OH-NVP to quinoid species is a plausible event, similar to what is observed with other phenolic metabolites and/or parent drugs; the electrophilic metabolites thus generated are widely thought to be involved in the toxicity of numerous xenobiotics.[32–34] To address the potential role of oxidation products from 2-OH-NVP in the adverse responses associated with NVP therapy, we investigated the oxidation of

Table 1 Experimental conditions used for the preliminary oxidation assays of 2-OH-NVP (10 mg, 35 μmol) with Frémy's salt or sodium periodate

Entry	Oxidant	Solvent A	Solvent B
1	Frémy's salt (12 mg, 45 μmol)	acetonitrile (800 μL)	100 mM phosphate (pH 10; 400 μL)
3		acetonitrile (800 μL)	100 mM phosphate (pH 7.4; 400 μL)
4		acetonitrile (800 μL)	100 mM phosphate (pH 5; 400 μL)
5		DMF (500 μL)	DMF (500 μL)
6	$NaIO_4$ (7.5 mg, 35 μmol)	acetonitrile (800 μL)	100 mM phosphate (pH 10; 400 μL)
7		acetonitrile (800 μL)	100 mM phosphate (pH 7.4; 400 μL)
8		acetonitrile (800 μL)	100 mM phosphate (pH 5; 400 μL)
9		DMF (500 μL)	DMF (500 μL)

this metabolite *in vitro* and characterized the major products. As model oxidants, we chose the radical potassium nitrosodisulfonate (Frémy's salt) and sodium periodate, which are frequently employed to obtain quinones from phenolic compounds.[46–48] The use of Frémy's salt has the advantage of mimicking the one-electron oxidation involved in enzyme-mediated metabolic oxidations[49,50] whereas periodate oxidation is thought to proceed by an ionic mechanism.[51]

Preliminary reactions with Frémy's salt were conducted at room temperature using 1.3 molar equivalents of the oxidant and a biphasic system of ethyl acetate and 100 mM phosphate buffer (pH 7.4 or 10). Due to the low solubility of 2-OH-NVP and the difficulty involved in HPLC monitoring of a biphasic mixture, alternative solvent systems were subsequently screened. These included DMF and acetonitrile/100 mM phosphate buffer at different pHs (5, 7.4, and 10). Sodium periodate oxidation assays were conducted under similar conditions, using equimolar amounts of oxidant and 2-OH-NVP (Table 1). In each instance, reactions were monitored by HPLC-DAD at least 1 and 24 h after addition of the oxidant. The yield of each product was calculated on the basis of the HPLC peak area, corrected for the corresponding molar absorptivity at the monitored wavelength (254 nm). For the purpose of spectroscopic characterization of the major products, larger scale reactions were performed and the products were isolated by semi-preparative HPLC or PTLC (*cf.* Experimental section).

Although the pattern of oxidation products was considerably affected by solvent and pH, spiro compounds [either **18** or **19** (**a**/**b**/**c**)] were always observed (Scheme 4; *vide infra* for the spectroscopic characterization). Despite the probable mechanistic differences, the formation of these spiro compounds, regardless of the oxidant used, suggests a fast generation of a transient electrophilic quinone-imine (**20**, Scheme 4), which was not detected. Interestingly, **18** was only observed when the oxidations were conducted in aqueous systems, whereas its isomer(s) **19** (**a**/**b**/**c**) appeared in DMF only (Fig. 1). The formation of the two spiro compounds can be explained on the basis of nucleophilic attack by water on positions C4a and C11a of the quinone-imine (**20**), yielding the ring-opened intermediates **21** and **22**, respectively, which subsequently underwent intramolecular ring closure to **18** and **19** (Scheme 4). In particular, the formation of **19** in DMF in the absence of added water can only be explained with involvement of a highly electrophilic intermediate (*i.e.*, the quinone-imine) that can readily react with the residual water present.

The reasons for the solvent-determined selectivity toward **18** or **19** are not entirely clear. When the oxidations were performed in DMF, besides the spiro tautomers **19**, we observed the formation of 2-(cyclopropylamino)nicotinic acid (**23**), most likely stemming from initial water attack on C4a of the quinone-imine to yield **21**, the nicotinamide precursor of the spiro compound **18**. However, possibly due to decreased availability of the amide nitrogen for nucleophilic attack as a result of strong DMF-nicotinamide association *via* hydrogen bonding,[52] intramolecular ring closure to give **18** did not occur. Instead, consecutive hydrolysis steps from **21** afforded the nicotinic acid **23**. This process presumably occurred with concomitant formation of 6-hydroxypyridine-2,3-dione (Scheme 4) and/or its tautomers, but these species were not detected, either due to further degradation or low intensity of the chromophores. By contrast, when the oxidations were performed in aqueous media we found no evidence for the formation of **19** or its putative precursor, the ring-opened species **22**. Steric hindrance caused by the cyclopropyl substituent may have been a factor in delaying initial nucleophilic attack on C11a of the quinone-imine, compared to attack on C4a. A higher rate of nucleophilic attack at C4a could plausibly shift the equilibria toward the formation of **18** in aqueous media, thus preventing the formation of **19**.

When the reactions were conducted in aqueous systems, the product profiles were considerably affected by the pH. For instance, in the presence of Frémy's salt, the major product formed after 1 h in basic medium (pH 10) was the spiro compound **18**; this material had nearly disappeared after 24 h, when the major product corresponded to the pyridopyrimidine derivative **24**, which had increased approximately 4-fold (Fig. 1 and Scheme 5). By contrast, the amount of the spiro derivative **18** formed after 1 h at pH 7.4 was *ca.* 4-fold lower than at pH 10 but remained essentially unchanged with time; under these conditions compound **24** was not detected (Fig. 1). Moreover, the amount of spiro compound **18** formed after 1 h at pH 5 was approximately 10- and 3-fold lower than at pH 10 and 7.4, respectively, but increased *ca.* 4-fold after 24 h; compound **24** was detected only in trace amounts after 24 h at pH 5 (Fig. 1). The overall oxidation efficiency with Frémy's salt was found to decrease in the order pH10 > pH7.4 > pH5. Taken together, these observations are consistent with the proposed mechanism for the formation of the spiro compound **18** (Scheme 4), involving a transient quinone-imine intermediate (**20**), which is expected to undergo base catalysis. The susceptibility of **18** to degradation in alkaline media also suggests base catalysis.

Contrasting with the results obtained with Frémy's salt, the formation of the spiro compound **18** was maximal at pH 5 in the presence of sodium periodate, indicating that periodic acid was the oxidant.[53] As such, there was a slight increase in the amount of the spiro compound **18** between 1 and 24 h at pH 5. While the extent of oxidation was low at both pH 7.4 and pH 10, the changes

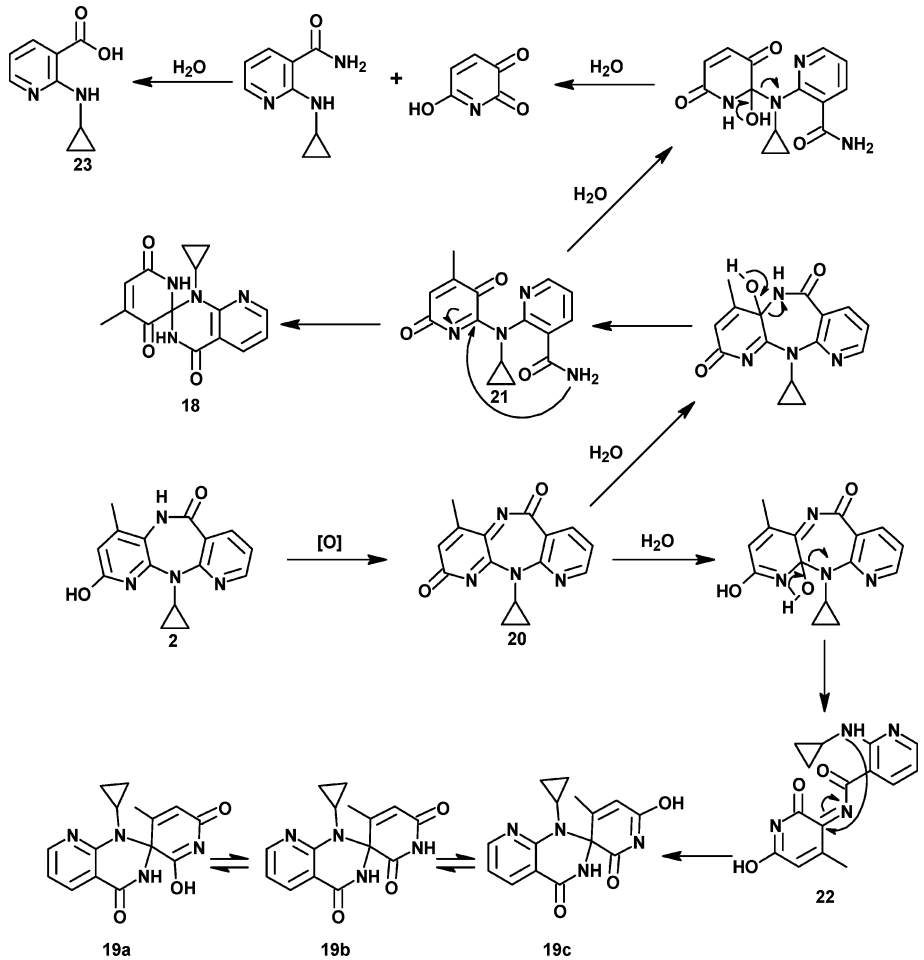

Scheme 4 Proposed mechanism for the formation of the spiro derivatives **18** and **19** and the nicotinic acid **23**, involving the transient generation of a quinone-imine (**20**). The spiro compound **18** was formed in aqueous solution only, and the spiro compound **19** was formed in DMF.

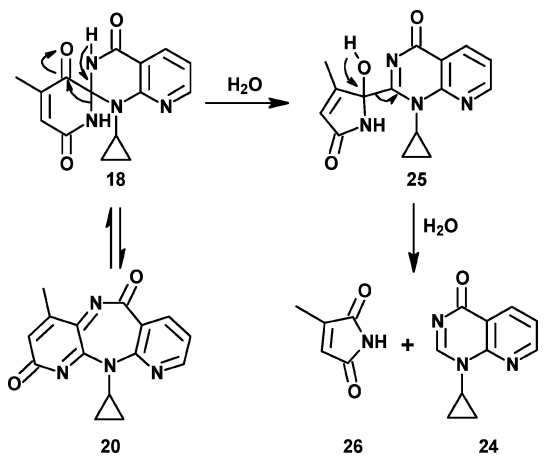

Scheme 5 Proposed mechanism for the hydrolytic degradation of the spiro compound **18**, leading to the irreversible formation of **24** and **26**.

in product profiles with time confirmed the stability of **18** in neutral media and its susceptibility to degradation at alkaline pH (Fig. 1).

To investigate further the degradation of **18** we isolated the compound and monitored its behaviour in solution, both in the absence and in the presence of Frémy's salt. Under the same solvent conditions, the results were identical with or without oxidant, which confirmed that oxidative processes were not involved. In DMF/100 mM phosphate buffer, pH 10 (Fig. 2) the pyridopyrimidine derivative **24** was already observed after 5 min of incubation; after 1 h, **18** and **24** were present in a ratio close to 1 : 1 and after 24 h, the conversion of **18** into **24** was almost complete (Fig. 2). Although this conversion was faster in basic medium, **24** was also detected after 1 h in DMF/phosphate buffer, pH 7.4; with longer incubation times (24 h) it was present in both DMF/phosphate buffer, pH 5, and DMF alone (Fig. 2). Interestingly, a residual amount of the spiro compound **18** was detected after 24 h at pH 10, but not pH 7.4, despite the lower rate of conversion at neutral pH (Fig. 2). This suggests some extent of competitive base-catalyzed reversible conversion of **18** to the ring-opened species **21** and/or the quinone-imine **20**, in a sequence of events mirroring the formation of **18** from **20** displayed in Scheme 4. Moreover, given the significant stability of **18** under mildly acidic conditions and in DMF, our observations are consistent with a base-catalyzed hydrolytic conversion of **18** to **24** (Scheme 5), presumably involving initial abstraction of the

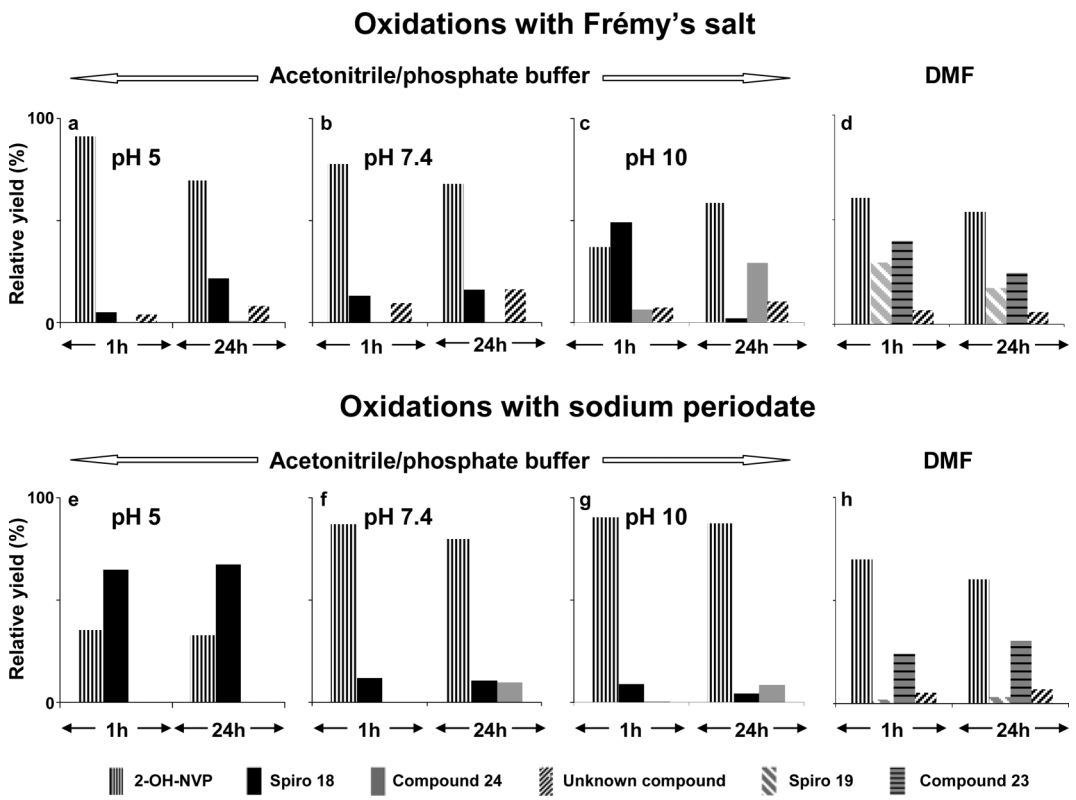

Fig. 1 Relative percentages of the compounds detected by HPLC-DAD in oxidation reactions of 2-OH-NVP, with Frémy's salt (panels **a**–**c** in acetonitrile/100 mM phosphate buffer at pH 5, 7.4, and 10, respectively; panel **d** in DMF) and sodium periodate (panels **e**–**g** in acetonitrile/100 mM phosphate buffer at pH 5, 7.4, and 10, respectively; panel **h** in DMF). The reactions were monitored at 254 nm and the quantifications were based on peak intensities, corrected for the molar absorptivities of the different compounds at 254 nm.

*N*3′-amide proton, with concomitant ring contraction to **25** and subsequent collapse of this intermediate to yield two stable species, **24** and the maleimide **26**. It should be noted that we were unable to detect **26** in any of the assays, probably due to low intensity of the chromophore at the wavelength (254 nm) used to monitor the reaction mixtures by HPLC-DAD.

In contrast to its isomer, the spiro derivative **19** (**a/b/c**) was very stable under the hydrolytic conditions used to study the degradation of **18**, both in the presence and in the absence of Frémy's salt (not shown). Solvent exposure of the *N*3′-amide proton may be lower in **19**, due to the vicinity of the methyl substituent, thus preventing the initiation of the process. However, it is more plausible that a base-catalyzed ring-contraction in **19** is not favoured because it would require cleavage of a C–C bond, rather than the C–N bond scission observed for **18**.

Enzyme-mediated oxidations

Lactoperoxidase, a member of the heme peroxidase family of enzymes, is secreted from mammary, salivary, and other mucosal glands and is known to catalyze the oxidation of a number of organic and inorganic substrates mediated by endogenous hydrogen peroxide.[54] It has been proposed that oxidation of the phenolic ring of estradiol by lactoperoxidase, with production of free radicals, may be involved in breast carcinogenesis.[55,56] In addition, it has been speculated that lactoperoxidase-catalyzed activation of xenobiotic carcinogens (*e.g.*, aromatic and heteroaromatic amines) could also be a factor in the initiation of breast cancer.[57]

Taking into consideration the phenol-type structure of 2-OH-NVP and the indirect evidence that an electrophilic quinone-imine (**20**) is an intermediate in the oxidation of this compound by both Frémy's salt and sodium periodate, we investigated if a similar transformation could occur under biologically plausible conditions. Toward this end, we incubated 2-OH-NVP with hydrogen peroxide in the presence of lactoperoxidase. The resulting mixture was analyzed by HPLC-DAD. By comparison of the retention times and distinctive UV profiles with those of the previously characterized standards, we could easily identify the pyridopyrimidine derivative **24** (Fig. 3, panels **A** and **B**). A signal with the retention time of the spiro compound **18**, not detected in the absence of lactoperoxidase, was also present; however, there were slight differences in the UV spectrum compared to the standard (not shown), possibly due to co-elution with another component of the mixture. To resolve this uncertainty, the incubation mixture was analyzed by LC-ESI-MS. Based upon retention time, detection of the protonated molecule (*m*/*z* 299), and MS/MS fragmentation pattern (Fig. 3, panels **C** and **D**), we obtained clear evidence for the formation of the spiro compound **18**. These results demonstrate that lactoperoxidase has the ability to catalyze the oxidation of 2-OH-NVP, yielding the same products obtained with Frémy's salt and sodium periodate. Moreover, the data support our initial hypothesis that the metabolism of NVP to 2-OH-NVP, and subsequent metabolic activation to **20**, is plausible *in vivo*, and could be a factor in some of the toxic events associated with NVP administration.

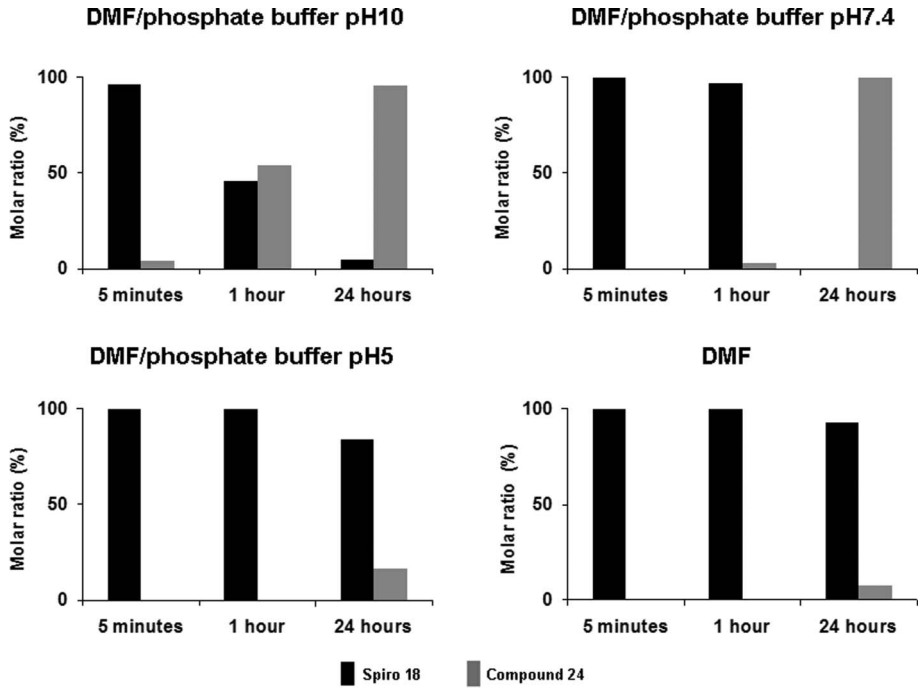

Fig. 2 Relative percentages of the compounds detected by HPLC-DAD during the stability assessment of the spiro compound **18** in different conditions. The reactions were monitored at 254 nm and the quantifications were based on peak intensities, corrected for the molar absorptivities of the different compounds at 254 nm.

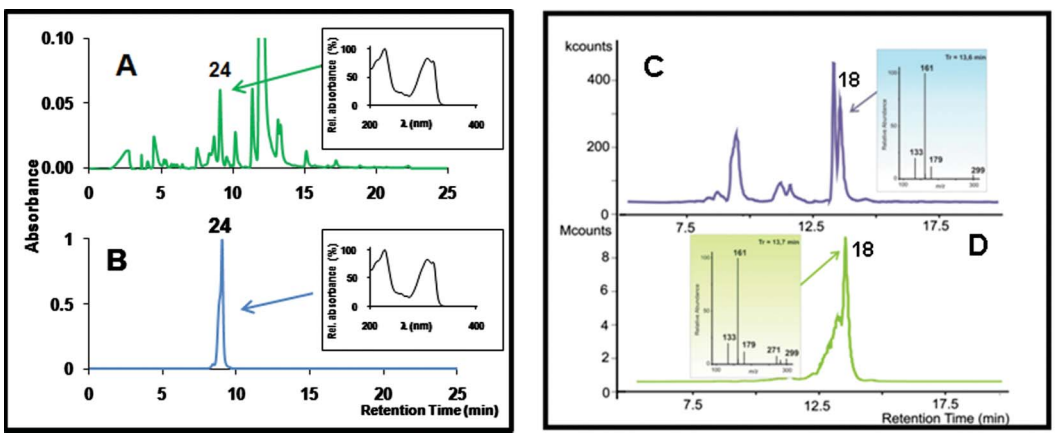

Fig. 3 HPLC-DAD chromatograms of: **A**) the reaction mixture obtained after incubation of 2-OH-NVP with lactoperoxidase; **B**) standard **24**; and LC-MS/MS spectra of the protonated spiro molecule **18** (*m*/*z* 299) in: **C**) the incubation mixture containing 2-OH-NVP and lactoperoxidase; **D**) the synthetic standard of the spiro compound.

Spectroscopic characterization of the oxidation products from 2-OH-NVP

An initial comparison of the ^{1}H and ^{13}C NMR spectra of all the products from 2-OH-NVP oxidation (*cf.* Experimental section) promptly allowed the conclusion that ring C (Scheme 1) remained unchanged in these derivatives, whereas a substantial degradation of rings A and B had occurred during the oxidation process.

The structural similarity between the two isomeric spiro compounds, **18** and **19**, was initially inferred during the HPLC-DAD separation process, whereupon the two compounds displayed very close retention times and similar UV profiles (Fig. 4). The ESI-MS spectra were consistent with isomers, exhibiting protonated molecules at *m*/*z* 299. Compound **19** had a greater propensity to be sodiated under the ionization conditions used, showing an intense $[M + Na]^{+}$ peak at *m*/*z* 321. The MS/MS spectra of the protonated molecules of both compounds yielded common product ions, as a result of preferential protonation of the basic pyridine nitrogen in both instances (*cf.* Scheme S1, Electronic Supplementary Material†).

The most distinctive feature in the NMR spectra of the spiro compounds was the presence of high field quaternary carbons (at 82.6 and 74.7 ppm, for **18** and **19**, respectively; *cf.* Experimental section and Electronic Supplementary Material†). This observation was the first evidence for a loss of aromaticity in ring A; moreover, the resonances obtained were compatible with spiro

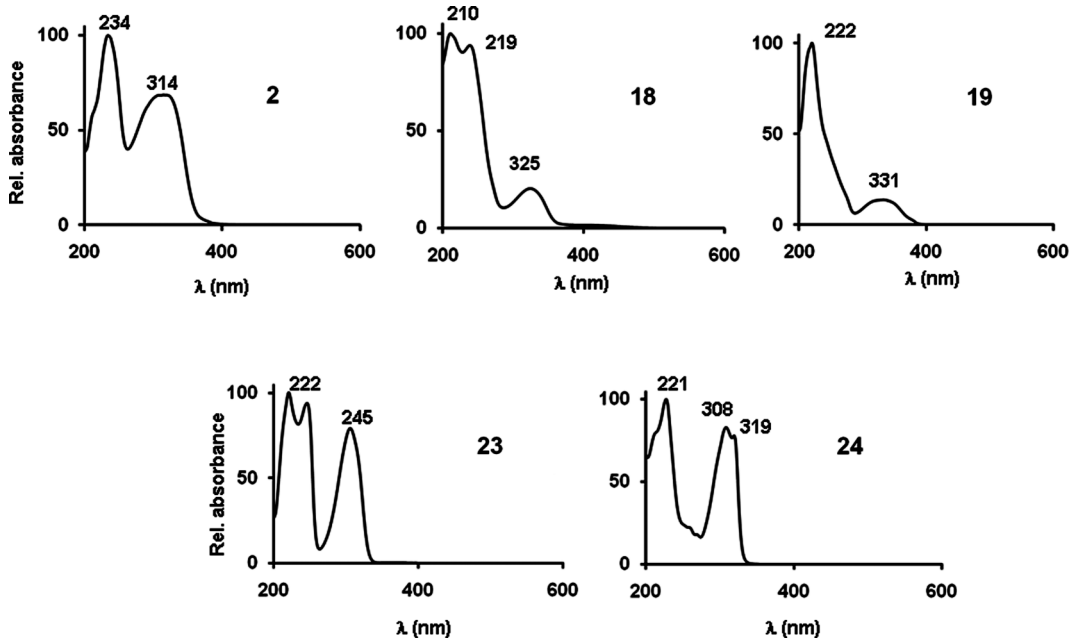

Fig. 4 UV spectra of 2-OH-NVP (**2**), the spiro compounds **18** and **19**, the nicotinic acid **23**, and compound **24**, isolated in oxidation reactions of 2-OH-NVP. The spectra were obtained online, by HPLC-DAD, in acetonitrile/0.1% aqueous formic acid.

quaternary carbons bound to at least one electron withdrawing substituent.[58] Although definite proof for the structure of **18** was obtained by X-ray diffraction (*vide infra*), it should be noted that this structure could be solved by analysis of the 2- and 3-bond HMBC ^{1}H-^{13}C correlations (Fig. 5). In particular, 2-bond correlations were observed between N3′H (9.04 ppm) and both the spiro quaternary carbon (C2; 82.6 ppm) and the amide C4′ (161.5 ppm); likewise, a 3-bond correlation between the same exchangeable proton and C4′a (111.3 ppm) was detected. Further crucial evidence was provided by the observation of 3-bond correlations between the exchangeable N1H and both the olefinic C5 (136.5 ppm) and the carbonyl C3 (191.2 ppm). All other proton and carbon resonances were consistent with the proposed structure.

The X-ray crystallographic data indicated that **18** crystallizes in the monoclinic *C*2/*c* space group: a = 21.528(10) Å; b = 8.433(4) Å; c = 17.211(8) Å; α = 90°; β = 94.650(16)°; γ = 90°; V = 3114(3) Å^3; Z = 4. After refinement the residual factor, R_1, had a value of 0.0591 (*cf.* Table S1, Electronic Supplementary Material†). The molecule is composed of two ring systems, a 6-membered ring and a bicyclic unit consisting of two fused 6-membered rings, with the two systems connected at C2 (Fig. 6). The figure shows the molecular structure of the *R*- enantiomer; it should be noted that, since *C*2/*c* is a centrosymmetric space group, the *S*- enantiomer is generated by symmetry operations. The average planes of the two rings display an angle of 78.63(7)°, a parameter that, together with the values of the angles between the 4 bonds originating at C2 [ranging from 106.5(2)° to 111.3(2)°)], confirms that the geometry around this atom is nearly tetrahedral. It is noteworthy that both the single 6-membered ring and the inner ring of the fused system show significant atomic deviations from planarity (–0.09225 to 0.1180 Å and –0.1522 to 0.2721 Å, respectively) and large bond length differences, due to the presence of sp^3 nitrogen atoms; on the contrary, the outer ring is planar and shows aromaticity, with similar values for all bond lengths. Bond lengths and angles (*cf.* Table S2, Electronic Supplementary Material†) are well within the expected range, as judged from extensive analysis of the values included in the Cambridge Structural Database (CSD).[59] The crystal structure of compound **18** revealed a solvent crystallization molecule (dimethylketone) for two molecules of compound. Fig. 7 displays the interactions between two molecules of **18** (one of isomer *R* and the other one of isomer *S*) and one solvent molecule. Thus, an $R^2_2(8)$ synthon is formed by N–H…O hydrogen bonds ($N1_{R/S}\cdots O9_{S/R}$ = 2.895 Å; $H1_{R/S}\cdots O9_{S/R}$ = 2.004 Å; $N1_{R/S}$ –$H1_{R/S}\cdots O9_{S/R}$ = 177.1°) between the two enantiomers. In addition, a short C–H…O contact with the solvent ($C_{methyl}\cdots O9$ = 3.378 Å; $H_{methyl}\cdots O9$ = 2.620 Å; C_{methyl}–$H_{methyl}\cdots O9$ = 134.2°) is also observed. Interaction between two molecules of the same enantiomer was seen as well, establishing another $R^2_2(8)$ synthon by N–H…O hydrogen bonds (N3′…O12′ = 2.862 Å; H3′…O12′ = 1.940 Å; N3′–H3′…O12′ = 164.6°) (*cf.* Electronic Supplementary Material†).

We were unable to obtain crystals of the spiro compound **19** suitable for X-ray diffraction analysis. Therefore, the definite structural assignment was based essentially on the ^{1}H-^{13}C HMBC correlations (Fig. 8). The proton signal at 6.23–6.25 ppm (H5) showed three-bond correlations with the methyl carbon (18.5 ppm) and the spiro quaternary carbon (C3; 74.7 ppm). Three-bond correlations were also observed between the methyl protons (2.14 ppm) and both the spiro carbon (C3; 74.7 ppm) and C5 (123.9 ppm). Based upon these correlations, and ignoring potential tautomerism in the pyrimidinone-type ring, three different tautomeric structures consistent with the data can be proposed for **19** (Scheme 4). Evidence for the co-existence of more than one isomer in equilibrium can be inferred from the presence of multiple resonances for a few specific signals in the ^{1}H and ^{13}C NMR spectra [*e.g.*, H5 (an apparent multiplet at 6.23–6.25 ppm), C4′ (164.8 and 164.9 ppm), and C2/C6 (169.5 and 169.6 ppm).

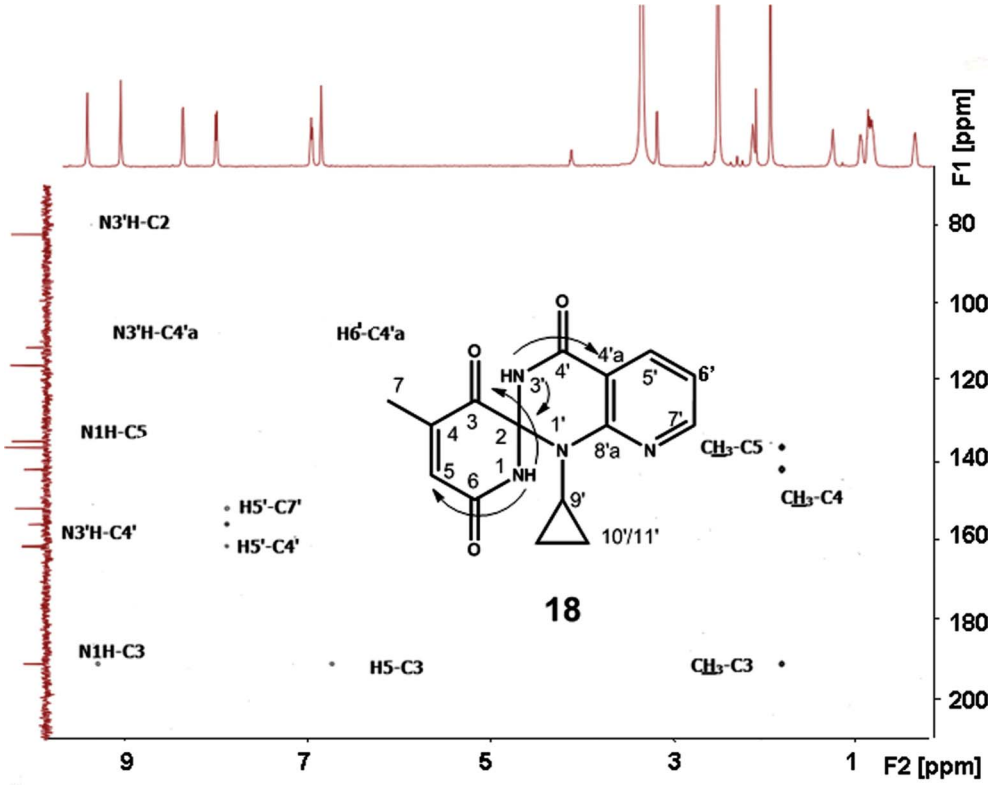

Fig. 5 Expanded region of the ^{1}H-^{13}C HMBC spectrum of the spiro compound **18**, displaying the 3-bond connectivities between the N1H proton and carbons C3 and C5, and the 2- and 3-bond connectivities between the N3′H proton and the spiro (C2) and C4′a carbons, respectively.

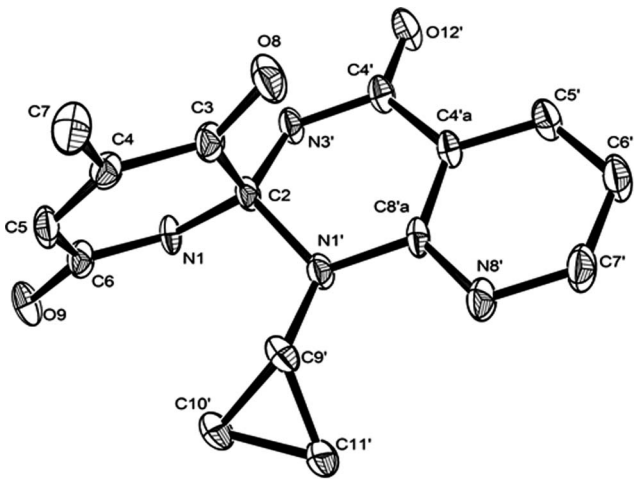

Fig. 6 ORTEP diagram, drawn with 50% probability ellipsoids, showing the atomic labelling scheme for the spiro compound **18**.

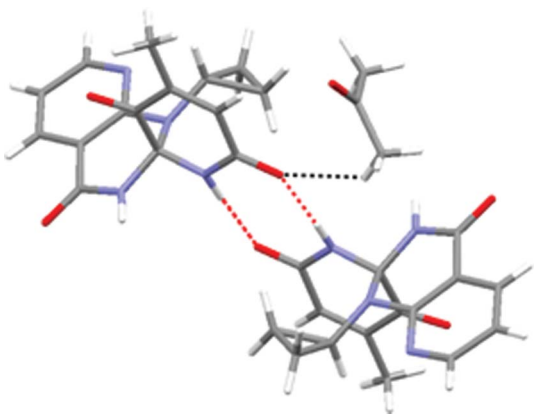

Fig. 7 Diagram displaying the interactions between two molecules of the spiro compound **18** (one of isomer *R*, left, and another of isomer *S*, right) and one molecule of solvent (dimethylketone).

The two C4′ resonances were identified on the basis of three-bond HMBC correlations with H5′ (8.07 ppm) but the C2 and C6 resonances could not be assigned unambiguously, due to the lack of HMBC correlations involving these quaternary carbons.

By comparison with the spiro compounds, the characterization of the pyridopyrimidine derivative **24** and of the nicotinic acid **23** was straightforward. A considerable decrease in the number of ^{13}C NMR signals in **24**, when compared to 2-OH-NVP, was the first evidence for the loss of ring A. Additionally, the presence of a one-proton singlet at 8.64 ppm, correlating with a carbon signal at 156.3 ppm in the ^{1}H-^{13}C HSQC spectrum, suggested the presence of an imine group in the molecule. Conclusive evidence for the structural assignment was obtained from the ^{1}H-^{13}C HMBC 3-bond correlations observed between H2 and the carbonyl C4 (170.2 ppm), the quaternary C8a (152.2 ppm), and the cyclopropyl C-9 (31.8 ppm) (*cf.* Experimental section and Electronic Supplementary Material†). Moreover, the ESI mass spectral data were entirely consistent with structure **24**;

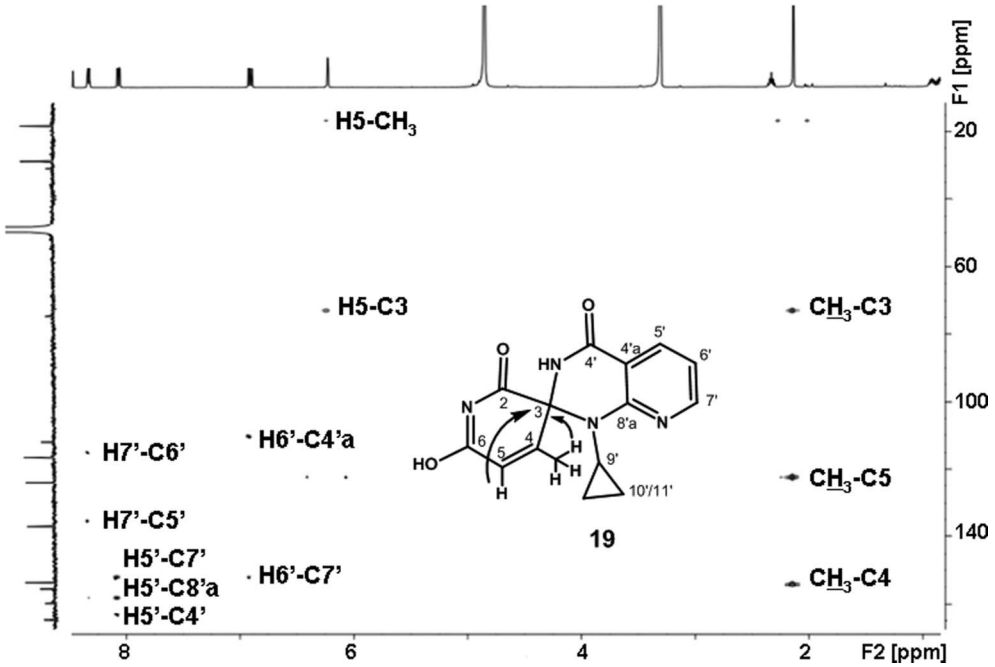

Fig. 8 Expanded region of the ^{1}H-^{13}C HMBC spectrum of the spiro compound **19**, displaying the 3-bond connectivities between the spiro carbon C3 and both the methyl and olefinic (H5) protons.

both the protonated (*m*/*z* 188) and sodiated (*m*/*z* 210) molecules were observed and MS/MS of the protonated molecule resulted in characteristic fragmentations, involving sequential loss of the cyclopropyl moiety, HCN and CO (*cf.* Scheme S2, Electronic Supplementary Material†).

The nicotinic acid **23** has previously been reported as a zwitterion[60] but the structural characterization data were not provided. We isolated this compound in very small amounts, which precluded obtaining a ^{13}C NMR spectrum with good signal/noise ratio. Nonetheless, carbon resonance assignments were performed on the basis of the correlations observed in the more sensitive inverse bidimensional experiments, HSQC and HMBC. The identification of **23** relied on the recognition of ^{1}H NMR signal patterns from a 2,3-disubstituted pyridine and a cyclopropylamino group (*cf.* Experimental section), which confirmed that the original ring C of 2-OH-NVP was essentially intact. A relevant three-bond correlation, observed in the ^{1}H-^{13}C HMBC spectrum between H4 (8.29 ppm) and a quaternary carbon at 162.4 ppm, indicated that a carbonyl group was still bound to the pyridine ring (not shown). Labile protons were not detected, presumably due to fast exchange on the NMR timescale, but the ESI mass spectrum yielded a signal at *m*/*z* 379, entirely consistent with a sodiated dimer of **23**. Given the presence of both an amino and a carboxylic acid group in the molecule, this propensity for dimerization was not unexpected.

Conclusions

The product profile obtained upon chemical and enzymatic oxidation of 2-OH-NVP is consistent with the formation of a transient quinone-imine intermediate (**20**). The presence of this electrophilic species in the reaction media supports the hypothesis that an activation pathway from phenolic NVP metabolites, in particular 2-OH-NVP, may play a role in NVP-induced toxicity. The toxicological significance of quinone-imine intermediates has long been recognized.[61] Representative examples of therapeutic drugs activated *via* quinone-imines are the analgesic acetaminophen (paracetamol),[62–64] the nonsteroidal antiinflammatory agent diclofenac,[65] and the cyclooxygenase-2 inhibitor lumiracoxib.[66,67] Indeed, an intermediate quinone-imine has been postulated to be at the onset of fatal liver damage prompted by overmedication with paracetamol, presumably due to covalent protein binding when the sacrificial detoxifying agent, glutathione, has been depleted.

Our data indicate that the intermediate quinone-imine **20** underwent prompt nucleophilic attack by water, which supports the likelihood of competitive reaction with bionucleophiles *in vivo*, affording covalent adducts. Quinone-imines are known to be especially prone to nucleophilic attack by sulfhydryl groups, and thus glutathione conjugation represents the typical detoxification process for these electrophiles.[68] However, given that HIV-infected patients are reported to have depleted levels of glutathione,[69] this will hamper an efficient detoxification of quinone-imine metabolites, which will conceivably become available to react with sulfhydryl groups (or other nucleophilic side chains) in proteins, eliciting toxic responses.

The most interesting end products of oxidative degradation of 2-OH-NVP were the spiro compounds **18** and **19**. Naturally occurring bioactive spiro compounds are well known,[70] and the generation of spiro derivatives as oxidation products from other drugs and toxicants has also been reported.[71,72] Considering that **19** only formed in non-aqueous media and proved to be stable under hydrolytic and oxidative conditions, it is not anticipated to have biological significance. On the contrary, **18** was formed in aqueous media, including under lactoperoxidase catalysis, and was very susceptible to hydrolysis, which suggests that it may be

prone to reacting with bionucleophiles. Although the significance of this pathway to toxicity remains to be established, the formation of electrophilic 2-OH-NVP derivatives under lactoperoxidase catalysis suggests that it could play a role in the perinatal setting, due to NVP administration concurrently with breastfeeding and the fact that nevirapine readily enters breast milk.[13]

Experimental

General remarks

Chemicals. NVP was purchased from Cipla (Mumbai, India). All other commercially available reagents and enzymes were acquired from Sigma-Aldrich Química, S.A. (Madrid, Spain), unless specified otherwise, and were used as received. Whenever necessary, solvents were purified by standard methods.[73]

Instrumentation. Melting temperatures were measured in a Leica Galen III hot stage apparatus and are uncorrected. Infrared (IR) spectra were recorded on a Perkin-Elmer 683IR spectrometer (Waltham, MA); group frequencies are reported in cm^{-1}. The UV measurements were recorded on a Perkin Elmer Lambda 35 UV/VIS spectrophotometer. HPLC was conducted on an Ultimate 3000 Dionex system consisting of an LPG-3400A quaternary gradient pump and a diode array spectrophotometric detector (Dionex Co., Sunnyvale, CA) and equipped with a Rheodyne model 8125 injector (Rheodyne, Rohnert Park, CA). HPLC analyses were performed with a Luna C18 (2) column (250 mm × 4.6 mm; 5 μm; Phenomenex, Torrance, CA), at a flow rate of 1 mL min^{-1}. Semipreparative HPLC separations were conducted with a Luna C18 (2) column (250 mm × 10 mm; 5 μm; Phenomenex) at a flow rate of 3 mL min^{-1}. A 30-min linear gradient from 5 to 70% acetonitrile in 0.1% aqueous formic acid, followed by a 2-min linear gradient to 100% acetonitrile and an 8-min isocratic elution with acetonitrile, was used in all instances. The UV absorbance was monitored at 254 nm.

LC-ESI-MS/MS analyses were performed with a Varian system consisting of a ProStar 410 autosampler, two 210-LC chromatography pumps, a ProStar 335 diode array detector, and a 500-MS ion trap mass spectrometer, with an ESI ion source (Varian, Inc., Palo Alto, CA). Data acquisition and processing were performed using Varian MS Control 6.9 software. The samples were injected onto the column *via* a Rheodyne injector with a 20 μL loop. Separations were conducted at 30 °C, using a Luna C18 (2) column (150 mm × 2 mm, 3 μm; Phenomenex). The mobile phase was delivered at a flow rate of 200 μL min^{-1}, using a 5-min isocratic elution with 5% acetonitrile in 0.1% aqueous formic acid, followed by a 30-min linear gradient from 5 to 70% acetonitrile, a 2-min linear gradient to 100% acetonitrile, and an 8-min isocratic elution with acetonitrile. The mass spectrometer was operated in the positive ESI mode; the optimized operating parameters were: ion spray voltage, +5.2 kV; capillary voltage, 20 V; and RF loading, 90%. Nitrogen was used as the nebulizing and drying gas, at pressures of 50 and 30 psi, respectively; the drying gas temperature was 350 °C. MS/MS spectra were obtained with an isolation window of 1.5 Da, excitation energy values between 0.9 and 1.2 V, and an excitation time of 10 ms. High resolution ESI mass spectra were obtained on a Bruker Apex Ultra FTICR mass spectrometer (Bruker Daltonics, Billerica, MA) at the FCUL node of the Portuguese MS network.

^{1}H NMR spectra were recorded on Bruker Avance III 400 or 500 spectrometers (Bruker BioSpin GmbH, Rheinstetten, Germany) operating at 400 and 500 MHz, respectively. ^{13}C NMR spectra were recorded on the same instruments, operating at 100.62 and 125.77 MHz, respectively. Chemical shifts are reported in ppm downfield from tetramethylsilane, and coupling constants (J) are reported in Hz; the subscripts *ortho* and *meta*, refer to *ortho* and *meta* couplings, respectively, and asterisks are used to indicate a second isomer. The presence of labile protons was confirmed by chemical exchange with D_2O. Resonance and structural assignments were based on the analysis of coupling patterns, including the ^{13}C-^{1}H coupling profiles obtained in bidimensional heteronuclear multiple bond correlation (HMBC) and heteronuclear single quantum coherence (HSQC) experiments, performed with standard pulse programs.

X-ray crystallographic data for compound **18** were collected from crystals using an area detector diffractometer (Bruker AXS-KAPPA APEX II) equipped with an Oxford Cryosystem open-flow nitrogen cryostat at 150 K and graphite-monochromated Mo-Kα ($\lambda = 0.71073$ Å) radiation. Cell parameters were retrieved using Bruker SMART software and refined with Bruker SAINT[74] on all observed reflections. Absorption corrections were applied using SADABS.[75] The structures were solved by direct methods using SIR 97[76] and refined with full-matrix least-squares refinement against F^2 using SHELXL-97.[77] All the programs are included in the WINGX package (version 1.70.01).[78] All non-hydrogen atoms were refined anisotropically, and the hydrogen atoms were inserted in idealized positions, riding on the parent C atom, except for the methyl hydrogens, whose orientation was refined from electron density, allowing the refinement of both C–C torsion angles and C–H distances, and the hydrogen atoms bonded to nitrogens, which were found directly in the density map. Drawings were made with ORTEP3 for Windows.[79] Intermolecular interactions were analysed using Mercury 1.4.2 (Build 2).[80] Plane calculations were made using Parst.[81,82] The crystals had reasonable quality and diffracting power, presenting low R_2 values (0.123) that allowed low R values ($R_{1\,all} = 0.139$ and $R_{1\,obs} = 0.059$). The structure was, therefore, unequivocally determined and is in good agreement with the remaining spectral characterization data for **18**. Relevant details of the X-ray data analysis are displayed in the Electronic Supplementary Material† section.

Synthesis of 11-cyclopropyl-2-hydroxy-4-methyl-5,11-dihydro-6*H*-dipyrido[3,2-*b*:2′,3′-*e*][1,4]diazepin-6-one (2-OH-NVP, 2)

11-Cyclopropyl-4-methyl-6-oxo-6,11-dihydro-5*H*-dipyrido[3,2-*b*:2′,3′-*e*][1,4]diazepin-2-yl acetate (2-acetoxy-NVP, 15). To a solution of NVP (250 mg, 0.94 mmol) in dichloromethane (100 mL) at 104 °C (temperature of the oil bath), were added silver acetate (1.25 g, 7.5 mmol) and then iodine (1.15 g, 4.5 mmol), and the resulting solution was stirred at 104 °C for 5 min. The yellow solid formed upon cooling to room temperature was applied onto a silica bed. Iodine was removed with dichloromethane and the product was eluted with ethyl acetate/dichloromethane (1 : 1; 150 mL) and recovered in quantitative yield upon evaporation. M_p = 242–245 °C (AcOEt); **IR (KBr)**: 1774 (C═O, ester), 1654 (C═O, amide); **^{1}H NMR ($CDCl_3$)**: δ 8.73 (1H, s, NH), 8.52 (1H, dd, J_{ortho} = 4.8 and J_{meta} = 1.8, H9), 8.10 (1H, dd, J_{ortho} = 7.8 and J_{meta} = 1.8, H7), 7.08 (1H, dd, J_{ortho} = 7.8 and J'_{ortho} = 4.8, H8), 6.73 (1H, s, H3),

3.69–3.67 (1H, m, H13), 2.41 (3H, s, C12H$_3$), 2.34 (3H, s, COCH$_3$), 0.98–0.96 (2H, m, H14+H15), 0.50–0.49 (2H, m, H14+H15); **^{13}C NMR (CDCl$_3$)**: δ 169.1 (OC═O), 168.6 (C6), 160.3 (C10a), 152.8 (C2/C11a), 152.6 (C2/C11a), 152.0 (C9), 142.7 (C4), 140.3 (C7), 123.0 (C4a), 120.1 (C6a), 119.0 (C8), 113.5 (C3), 29.5 (C13), 21.2 (CO$\underline{C}$H$_3$), 18.1 (C12), 8.9 (C14 + C15); **MS (ESI)**: *m/z* 347 [M + Na]$^+$, 325 [MH]$^+$, 283 [MH$_2$ – COCH$_3$]$^+$. **HRMS** calcd for [C$_{17}$H$_{16}$N$_4$O$_3$ + H]$^+$: 325.129517. Found: 325.12941.

2-OH-NVP (2). The entire amount of **15** (*ca.* 0.94 mmol), obtained as described above, was dissolved in methanol (10 mL), 10% KOH was added to the solution, and the mixture was stirred at room temperature for 15 min. The methanol was then evaporated and the pH was adjusted to 7, allowing the precipitation of a white solid, which was isolated by centrifugation and washed with ethanol to afford **2** (225 mg, 0.80 mmol, 85% overall yield). M_p = 330–332 °C (ethanol) (lit.[36] >270 °C); **IR (KBr)**: 3195 (O–H and N–H), 1654 (C═O); **UV (acetonitrile)**: λ_{max} 234, 314 nm; **^{1}H NMR (DMSO-*d*$_6$)**: δ 10.56 (1H, bs, OH), 9.60 (1H, s, NH), 8.47–8.46 (1H, m, H9), 7.97–7.95 (1H, m, H7), 7.16–7.13 (1H, m, H8), 6.29 (1H, s, H3), 3.55 (1H, bs, H13), 2.22 (3H, s, CH$_3$), 0.85 (2H, bs, H14 + H15), 0.35 (2H, bs, H14 + H15); **^{13}C NMR (DMSO-d$_6$)**: δ 167.4 (C6), 160.8 (C10a), 159.8 (C2), 152.4 (C11a), 151.3 (C9), 145.0 (C4), 140.3 (C7), 121.6 (C6a), 119.6 (C8), 117.6 (C4a), 106.9 (C3), 29.2 (C13), 18.2 (CH$_3$), 9.0 (C14/C15), 8.9 (C14/C15); **MS (EI)**: ***m/z*** 282 [M]$^+$ (76.7%), 281 [M – H]$^+$ (100.0%), 267 [M – CH$_3$]$^+$ (60.4%), 253 [M – HCO]$^+$ (30.3%).

Oxidations of 2-OH-NVP

General method for preliminary reactions with Frémy's salt and sodium periodate. To a solution of 2-OH-NVP (10 mg, 35.5 µmol) in solvent A was added a solution of the oxidant in solvent B (Table 1). The reaction mixture was monitored by HPLC-DAD at 254 nm after 1 and 24 h.

Reaction with lactoperoxidase. To a solution of 2-OH-NVP (10 mg, 35.5 µmol) in 100 mM phosphate, pH 7.4 (200 µL) were added a solution of hydrogen peroxide (0.5%, 50 µL) and a solution of lactoperoxidase (EC 1.11.1.7; 0.4–0.7 units mL^{-1} in 100 mM phosphate, pH 7.4; 14 µL). The resulting mixture was incubated overnight at 37 °C and then analyzed by LC-DAD and LC-MS. A control assay was performed using the same conditions in the absence of lactoperoxidase.

Oxidation reactions on a preparative scale

With Frémy's salt in phosphate buffer. To a solution of 2-OH-NVP (40 mg, 142 µmol) in ethyl acetate (8 mL) was added a solution of Frémy's salt (48 mg, 179 µmol) in 100 mM phosphate buffer (4 mL; pH 5, 7.4, or 10) and the mixture was stirred overnight at room temperature. Following phase separation and additional extraction with ethyl acetate, the organic layers were dried over anhydrous sodium sulfate and the products were isolated by PTLC on silica (1/1 dichloromethane/ethyl acetate). The novel products characterized from these reactions were:

At pH 7.4

1′-Cyclopropyl-4-methyl-1*H*,1′*H*-spiro[pyridine-2,2′-pyrido[2,3-*d*]pyrimidine]-3,4′,6(3′*H*)-trione (18). Obtained in 7% yield (3 mg); M_p = 172–174 °C; **Retention time** (R_t) = 13.2 min; **UV (acetonitrile)**: λ_{max} 210, 219, 325 nm; **^{1}H NMR (DMSO-*d*$_6$)**: δ 9.41 (1H, s, N1H), 9.04 (1H, s, N3′H), 8.36 (1H, d, J_{ortho} = 3.8, H7′), 8.00 (1H, d, J_{ortho} = 7.1, H5′), 6.97–6.94 (1H, m, H6′), 6.85 (1H, s, H5), 2.12–2.09 (1H, m, H9), 1.93 (3H, s, CH$_3$), 0.95–0.87 (1H, m, H10/H11), 0.87–0.81 (2H, m, H10/H11), 0.36–0,35 (1H, m, H10/H11); **^{13}C NMR (DMSO-*d*$_6$)**: δ 191.2 (C3), 161.6 (C6), 161.5 (C4′), 156.0 (C8′a), 151.9 (C7′), 142.1 (C4), 136.5 (C5), 135.0 (C5′), 115.7 (C6′), 111.3 (C4′a), 82.6 (C2), 25.8 (C9), 14.3 (CH$_3$), 9.1 (C10/C11), 8.4 (C10/C11). **MS (ESI)**: *m/z* 299 [MH]$^+$. **HRMS** calcd for [C$_{15}$H$_{14}$N$_4$O$_3$ + H]$^+$: 299.113867. Found: 299.11375. For the X-ray diffraction data see the Results and Discussion and Electronic Supplementary Material† section.

At pH 10:

Compound **18**, obtained in 8.3% yield (3.5 mg); and

1-Cyclopropylpyrido[2,3-*d*]pyrimidin-4(1*H*)-one (24). Obtained in 10.5% yield (2.8 mg); M_p = 210 °C; R_t, 9.3 min; **UV (acetonitrile)**: λ_{max} 221, 309, 319 nm; **^{1}H NMR (DMSO-*d*$_6$)**: δ 8.91 (1H, dd, J_{ortho} = 4.6 and J_{meta} = 1.9, H7), 8.64 (1H, s, H2), 8.43 (1H, dd, J_{ortho} = 7.8 and J_{meta} = 1.9, H5), 7.61 (1H, dd, J_{ortho} = 7.8 and J'_{ortho} = 4.6, H6), 3.54–3.48 (1H, m, H9), 1.23–1.04 (4H, m, H10 + H11); **^{13}C NMR (DMSO-*d*$_6$)**: δ 170.2 (C4), 156.3 (C2), 154.9 (C7), 152.2 (C8a), 137.8 (C5), 123.6 (C6), 115.8 (C4a), 31.8 (C9), 7.4 (C10 + C11); **MS (ESI)**: *m/z* 210 [M + Na]$^+$, 188 [MH]$^+$. **HRMS** calcd for [C$_{10}$H$_9$N$_3$O + H]$^+$: 188.081838. Found: 188.08150.

With Frémy's salt in DMF. To a solution of 2-OH-NVP (60 mg, 213 µmol) in DMF (3 mL) was added a solution of Frémy's salt (74 mg, 276 µmol) in DMF (3 mL). Following incubation at room temperature for 24 h, the mixture was purified by semi-preparative HPLC, yielding:

1′-Cyclopropyl-4-methyl-1′*H*,2*H*-spiro[pyridine-3,2′-pyrido[2,3-*d*]pyrimidine]-2,4′,6(1*H*,3′*H*)-trione [19 (a/b/c)]. Obtained in 3% yield (2 mg); M_p > 300 °C; R_t, 13.5 min; **UV (acetonitrile)**, λ_{max} 222, 331 nm; **^{1}H NMR (methanol-*d*$_4$)**: δ 8.33 (1H, dd, J_{ortho} = 5.0 and J_{meta} = 2.0, H7′), 8.07 (1H, dd, J_{ortho} = 7.5 and J_{meta} = 2.0, H5′), 6.91 (1H, dd, J_{ortho} = 7.5 and J'_{ortho} = 5.0, H6′), 6.25–6.23 (1H, m, H5), 2.36–2.30 (1H, m, H9′), 2.14 (3H, s, CH$_3$), 0.95–0.81 (2H, m, H10′/H11′), 0.75–0.73 (2H, m, H10′/H11′); **^{13}C NMR (methanol-*d*$_4$)**: δ 173.3 (C2/C6), 169.6 (C2/C6), 169.5 (C2*/C6*), 164.9 (C4′), 164.8 (C4′*), 159.8 (C8′a), 155.7 (C4), 153.5 (C7′), 137.0 (C5′), 123.9 (C5), 116.6 (C6′), 112.0 (C4′a), 74.7 (C3), 28.8 (C9′), 18.5 (CH$_3$), 9.0 (C10′/C11′), 8.9 (C10′/C11′). **MS (ESI)** *m/z* 321 [M + Na]$^+$, 299 [MH]$^+$. **HRMS** calcd for [C$_{15}$H$_{14}$N$_4$O$_3$ + H]$^+$: 299.113867. Found: 299.11388.

2-(Cyclopropylamino)pyridine-3-carboxylic acid (23). Obtained in 4% yield (1.5 mg); R_t = 12.0 min. **UV (acetonitrile)**: λ_{max} 222, 245 nm; **^{1}H RMN (DMSO-*d*$_6$)**: δ 8.73 (1H, dd, J_{ortho} = 4.7 and J_{meta} = 1.6, H6), 8.29 (1H, J_{ortho} = 7.7 and J_{meta} = 1.6, H4), 7.31 (1H, J_{ortho} = 7.7 and J'_{ortho} = 4.7, H5), 2.78–2.76 (1H, m, H8), 1.12–1.08 (2H, m, H9 + H10) 0.81–0.75 (2H, m, H9 + H10); **MS (ESI)**: *m/z*: 379 [2 M + Na]$^+$.

With sodium periodate. To a solution of 2-OH-NVP (60 mg, 213 µmol) in DMF (3 mL) was added a solution of NaIO$_4$ (45 mg, 210 µmol) in DMF (3 mL). Following incubation at room

temperature for 24 h, the mixture was purified by semi-preparative HPLC affording the spiro compound **19** in 1.5% yield (1 mg).

Assessment of the stability of the spiro compounds (18 and 19). To a solution of the spiro compound (**18** or **19**; 1.5 mg; 5 μmol) in DMF (100 μl) were added 100 μl of DMF or 100 mM phosphate buffer (pH 5, 7.4, or 10). A similar assay was performed in DMF in the presence of Frémy's salt. The resulting mixtures were monitored by HPLC after 5 min, 1 h, and 24h.

Abbreviations. CART, combined antiretroviral therapy; CYP, cytochrome P450; DMF, *N*,*N*-dimethylformamide; ESI, electrospray ionization; Frémy's salt, potassium nitrosodisulfonate; HIV, human immunodeficiency virus type 1; HPLC-DAD, high performance liquid chromatography with diode array detection; MS/MS, tandem mass spectrometry; NNRTI, non-nucleoside reverse transcriptase inhibitor; NVP, nevirapine; PTLC, preparative thin layer chromatography.

Acknowledgements

We thank the Portuguese NMR Network (IST-UTL Center) and the Portuguese MS Network (IST-UTL Center) for providing access to the facilities. This work was supported in part by Fundação para a Ciência e a Tecnologia (FCT), Portugal, through pluriannual funds to Centro de Química Estrutural (PEst-OE/QUI/UI0100/2011) and research grants PPCDT/QUI/56582/2004 and PTDC/QUI-QUI/113910/2009, and by Interagency Agreement Y1ES1027 between the National Center for Toxicological Research/Food and Drug Administration and the National Institute of Environmental Health Sciences/National Toxicology Program. The opinions expressed in this paper do not necessarily represent those of the U.S. Food and Drug Administration.

Notes and references

1 F. Vidal, F. Gutiérrez, M. Gutiérrez, M. Olona, V. Sánchez, G. Mateo, J. Peraire, C. Viladés, S. Veloso, M. López-Dupla and P. Domingo, *AIDS Rev.*, 2010, **12**, 15.
2 A. Calmy, B. Hirschel, D. A. Cooper and A. Carr, *Lancet*, 2007, **370**, 12.
3 C. J. Fichtenbaum, *Current HIV/AIDS Reports*, 2010, **7**, 92.
4 World Health Organization, WHO guidelines on HIV/AIDS (http://www.who.int/rpc/guidelines/hiv_aids/en/index.html; accessed May 16, 2011).
5 Food and Drug Administration, FDA approves nevirapine to treat HIV. 1996, *News release T96-44*, June 24, 1996.
6 M. A. Thompson, J. A. Aberg, P. Cahn, J. S. G. Montaner, G. Rizzardini, A. Telenti, J. M. Gatell, H. F. Günthard, S. M. Hammer, M. S. Hirsch, D. M. Jacobsen, P. Reiss, D. D. Richman, P. A. Volberding, P. Yeni and R. T. Schooley, *JAMA*, 2010, **304**, 321.
7 Panel on Treatment of HIV-Infected Pregnant Women and Prevention of Perinatal Transmission. Recommendations for Use of Antiretroviral Drugs in Pregnant HIV-1-Infected Women for Maternal Health and Interventions to Reduce Perinatal HIV Transmission in the United States. May 24, 2010; pp 1–117. Available at http://aidsinfo.nih.gov/ContentFiles/PerinatalGL.pdf. Accessed May 16, 2011.
8 E. Marseille, J. G. Kahn, F. Mmiro, L. Guay, P. Musoke, M. G. Fowler and J. B. Jackson, *Lancet*, 1999, **354**, 803.
9 J. B. Jackson, P. Musoke, T. Fleming, L. A. Guay, D. Bagenda, M. Allen, C. Nakabiito, J. Sherman, P. Bakaki, M. Owor, C. Ducar, M. Deseyve, A. Mwatha, L. Emel, C. Duefield, M. Mirochnick, M. G. Fowler, L. Mofenson, P. Miotti, M. Gigliotti, D. Bray and F. Mmiro, *Lancet*, 2003, **362**, 859.
10 M. Lallemant, G. Jourdain, S. Le Coeur, J. Y. Mary, N. Ngo-Giang-Huong, S. Koetsawang, S. Kanshana, K. McInstosh and V. Thaineua, for the Perinatal HIV Prevention Trial (Thailand) Investigators, *N. Engl. J. Med.*, 2004, **351**, 217.
11 S. Lockman, R. L. Shapiro, L. M. Smeaton, C. Wester, I. Thior, L. Stevens, F. Chand, J. Makhema, C. Moffat, A. Asmelash, P. Ndase, P. Arimi, E. van Widenfelt, L. Mazhani, V. Novitsky, S. Lagakos and M. Essex, *N. Engl. J. Med.*, 2007, **356**, 135.
12 FDA, Approval of Viramune XR (nevirapine) 400 mg extended release tablet, 2011 (http://www.fda.gov/ForConsumers/ByAudience/ForPatientAdvocates/HIVandAIDSActivities/ucm248800.htm; accessed May 16, 2011).
13 M. Mirochnick, D. F. Clarke and A. Dorenbaum, *Clin. Pharmacokinet.*, 2000, **39**, 281.
14 Six Week Extended-Dose Nevirapine (SWEN) Study Team, *Lancet*, 2008, **372**, 300.
15 M. S. Baylor and R. Johann-Liang, *J. Acquir. Immune Defic. Syndr.*, 2004, **35**, 538.
16 M. Popovic, J. M. Shenton, J. Chen, A. Baban, T. Tharmanathan, B. Mannargudi, D. Abdulla and J. P. Uetrecht, *Handb. Exp. Pharmacol.*, 2010, **196**, Part 3, 437.
17 VIRAMUNE® (nevirapine), *Physicians' Desk Reference*, 2009, 63rd ed, pp 873–881, Physicians' Desk Reference Inc., Montvale, NJ.
18 T. Powles, D. Robinson, J. Stebbing, J. Shamash, M. Nelson, B. Gazzard, S. Mandelia, H. Møller and M. Bower, *J. Clin. Oncol.*, 2009, **27**, 884.
19 P. Claes, M. Wintzen, S. Allard, P. Simons, A. De Coninck and P. Lacor, *Eur. J. Intern. Med.*, 2004, **15**, 255.
20 P. Riska, M. Lamson, T. MacGregor, J. Sabo, S. Hattox, J. Pav and J. Keirns, *Drug. Metab. Dispos.*, 1999, **27**, 895.
21 P. S. Riska, D. P. Joseph, R. M. Dinallo, W. C. Davidson, J. J. Keirns and S. E. Hattox, *Drug. Metab. Dispos.*, 1999, **27**, 1434.
22 D. A. Erickson, G. Mather, W. F. Trager, R. H. Levy and J. J. Keirns, *Drug. Metab. Dispos.*, 1999, **27**, 1488.
23 Z. Liu, P. Fan-Havard, Z. Xie, C. Ren and K. K. Chan, *Rapid Commun. Mass Spectrom.*, 2007, **21**, 2734.
24 C. Ren, P. Fan-Havard, N. Schlabritz-Loutsevitch, Y. Ling, K. K. Chan and Z. Liu, *Biomed. Chromatogr.*, 2010, **24**, 717.
25 J. Chen, B. M. Mannargudi, L. Xu and J. Uetrecht, *Chem. Res. Toxicol.*, 2008, **21**, 1862.
26 J. M. Shenton, M. Teranishi, M. S. Abu-Asab, J. A. Yager and J. P. Uetrecht, *Chem. Res. Toxicol.*, 2003, **16**, 1078.
27 B. Wen, Y. Chen and W. L. Fitch, *Drug Metab. Dispos.*, 2009, **37**, 1557.
28 A. M. M. Antunes, M. P. Duarte, P. P. Santos, G. Gamboa da Costa, T. M. Heinze, F. A. Beland and M. M. Marques, *Chem. Res. Toxicol.*, 2008, **21**, 1443.
29 A. M. M. Antunes, A. L. A. Godinho, I. L. Martins, G. C. Justino, F. A. Beland and M. M. Marques, *Chem. Res. Toxicol.*, 2010, **23**, 888.
30 A. M. M. Antunes, A. L. A. Godinho, I. L. Martins, M. C. Oliveira, R. A. Gomes, A. V. Coelho, F. A. Beland and M. M. Marques, *Chem. Res. Toxicol.*, 2010, **23**, 1714.
31 A. Srivastava, L.-Y. Lian, J. L. Maggs, M. Chaponda, M. Pirmohamed, D. P. Williams and B. K. Park, *Drug Metab. Dispos.*, 2010, **38**, 122.
32 J. L. Bolton, M. A. Trush, T. M. Penning, G. Dryhurst and T. J. Monks, *Chem. Res. Toxicol.*, 2000, **13**, 135.
33 T. J. Monks and D. C. Jones, *Curr. Drug Metab.*, 2002, **3**, 425.
34 S. Bittner, *Amino Acids*, 2006, **30**, 205.
35 K. G. Grozinger, D. P. Byrne, L. J. Nummy, M. D. Ridges and A. Salvagno, *J. Heterocyclic Chem.*, 2000, **37**, 229.
36 R. C. Cambie, G. J. Potter, P. S. Rutledge and P. D. Woodgate, *J. Chem. Soc., Perkin Trans. 1*, 1977, 530.
37 A. D'Alfonso, M. Pasi, A. Porta, G. Zanoni and G. Vidari, *Org. Lett.*, 2010, **12**, 596.
38 E. Ciganek and J. C. Calabrese, *J. Org. Chem.*, 1995, **60**, 4439.
39 W. Zhang, M. N. Wicks and P. L. Burn, *Org. Biomol. Chem.*, 2008, **6**, 879.
40 M. Iglesias, O. Schuster and M. Albrecht, *Tetrahedron Lett.*, 2010, **51**, 5423.
41 S. Aronson, P. Epstein, D. B. Aronson and G. Wieder, *J. Phys. Chem.*, 1982, **86**, 1035.
42 J. R. Barnett, L. J. Andrews and R. M. Keefer, *J. Am. Chem. Soc.*, 1972, **94**, 6129.
43 T. R. Beebe, B. A. Barnes, K. A. Bender, A. D. Halbert, R. D. Miller, M. L. Ramsay and M. W. Ridenour, *J. Org. Chem.*, 1975, **40**, 1992.
44 S. Rozen, D. Hebel and D. Zamir, *J. Am. Chem. Soc.*, 1987, **109**, 3789.

45 D. Hebel and S. Rozen, *J. Org. Chem.*, 1991, **56**, 6298.
46 J. G. Marrero, L. San Andrés and J. G. Luis, *Chem. Pharm. Bull.*, 2005, **53**, 1524.
47 J. M. Saá, J. Morey and C. Rubido, *J. Org. Chem.*, 1986, **51**, 4471.
48 M. Sugumaran, *Arch. Biochem. Biophys.*, 2000, **378**, 404.
49 H. Zimmer, D. C. Lankin and S. W. Horgan, *Chem. Rev.*, 1971, **71**, 229.
50 J. Zielonka, H. Zhao, Y. Xu and B. Kalyanaraman, *Free Radical Biol. Med.*, 2005, **39**, 853.
51 E. Adler and R. Magnusson, *Acta Chem. Scand.*, 1959, **13**, 505.
52 A. Johnston, A. J. Florence and A. R. Kennedy, *Acta Crystallogr., Sect. E: Struct. Rep. Online*, 2005, **61**, o1509.
53 S. W. Weidman and E. T. Kaiser, *J. Am. Chem. Soc.*, 1966, **88**, 5820.
54 H. Kohler and H. Jenzer, *Free Radical Biol. Med.*, 1989, **6**, 323.
55 H. J. Sipe Jr., S. J. Jordan, P. M. Hanna and R. P. Mason, *Carcinogenesis*, 1994, **15**, 2637.
56 E. M. Ghibaudi, E. Laurenti, P. Beltramo and R. P. Ferrari, *Redox Rep.*, 2000, **5**, 229.
57 K. M. Gorlewska-Roberts, C. H. Teitel, J. O. Lay Jr., D. W. Roberts and F. F. Kadlubar, *Chem. Res. Toxicol.*, 2004, **17**, 1659.
58 A. S. Kyei, K. Tchabanenko, J. E. Baldwin and R. M. Adlington, *Tetrahedron Lett.*, 2004, **45**, 8931.
59 F. H. Allen, O. Kennard, D. G. Watson, L. Brammer, A. G. Orpen and R. Taylor, *J. Chem. Soc., Perkin Trans. 2*, 1987, S1.
60 R. F. Boswell, B. F. Gupton and Y. S. Lo, *United States Patent* 6,680,383, 2004.
61 D. Porubek, M. Rundgren, R. Larsson, E. Albano, D. Ross, S. D. Nelson and P. Moldéus, *Adv. Exp. Med. Biol.*, 1986, **197**, 631.
62 I. A. Blair, A. R. Boobis and D. S. Davies, *Tetrahedron Lett.*, 1980, **21**, 4947.
63 W. Chen, L. L. Koenigs, S. J. Thompson, R. M. Peter, A. E. Rettie, W. F. Trager and S. D. Nelson, *Chem. Res. Toxicol.*, 1998, **11**, 295.
64 L. P. James, P. R. Mayeux and J. A. Hinson, *Drug Metab. Dispos.*, 2003, **31**, 1499.
65 J. S. van Leeuwen, G. Vredenburg, S. Dragovic, T. F. J. Tjong, J. C. Vos and N. P. E. Vermeulen, *Toxicol. Lett.*, 2011, **200**, 162.
66 Y. Li, J. G. Slatter, Z. Zhang, Y. Li, G. A. Doss, M. P. Braun, R. A. Stearns, D. C. Dean, T. A. Baillie and W. Tang, *Drug Metab. Dispos.*, 2008, **36**, 469.
67 P. Kang, D. Dalvie, E. Smith and M. Renner, *Chem. Res. Toxicol.*, 2009, **22**, 106.
68 D. J. Waldon, Y. Teffera, A. E. Colletti, J. Liu, D. Zurcher, K. W. Copeland and Z. Zhao, *Chem. Res. Toxicol.*, 2010, **23**, 1947.
69 D. M. Townsend, K. D. Tew and H. Tapiero, *Biomed. Pharmacother.*, 2003, **57**, 145.
70 R. Pradhan, M. Patra, A. K. Behera, B. K. Mishra and R. K. Behera, *Tetrahedron*, 2006, **62**, 779.
71 E. J. Land, A. Perona, C. A. Ramsden and P. A. Riley, *Org. Biomol. Chem.*, 2005, **3**, 2387.
72 M. Dračínský, J. Cvačka, M. Semanská, V. Martínek, E. Frei and M. Stiborová, *Chem. Res. Toxicol.*, 2009, **22**, 1765.
73 D. D. Perrin and W. L. F. Armarego, 1988, *Purification of Laboratory Chemicals*, 3rd ed., pp 1–391, Pergamon Press, Oxford, U. K.
74 *SMART and SAINT*: Area Detector Control and Integration Software, Bruker AXS, Madison, WI, USA, 2004.
75 G. M. Sheldrick, *SADABS*, Program for Empirical Absorption Correction of Area Detectors (Version 2.10), University of Göttingen, Germany, 2004.
76 A. Altomare, M. C. Burla, M. Camalli, G. L. Cascarano, C. Giacovazzo, A. Guagliardi, A. G. G. Moliterni, G. Polidori and R. Spagna, *J. Appl. Crystallogr.*, 1999, **32**, 115.
77 G. M. Sheldrick, *SHELXL-97*, a Computer Program for the Refinement of Crystal Structures, University of Göttingen, Göttingen, Germany, 1997.
78 L. J. Farrugia, *J. Appl. Crystallogr.*, 1999, **32**, 837.
79 L. J. Farrugia, *J. Appl. Crystallogr.*, 1997, **30**, 565.
80 I. J. Bruno, J. C. Cole, P. R. Edgington, M. Kessler, C. F. Macrae, P. McCabe, J. Pearson and R. Taylor, *Acta Crystallogr., Sect. B: Struct. Sci.*, 2002, **58**, 389.
81 M. Nardelli, *Comput. Chem.*, 1983, **7**, 95.
82 M. Nardelli, *J. Appl. Crystallogr.*, 1995, **28**, 659.